6-1-2015

Observer-Based Sliding Mode Control of Rijke-Type Combustion Instability

Jaime Rubio-Hervas
Nanyang Technological University, Singapore

Mahmut Reyhanoglu
Embry-Riddle Aeronautical University, reyhanom@erau.edu

William MacKunis
Embry-Riddle Aeronautical University, mackuniw@erau.edu

JOURNAL OF LOW FREQUENCY NOISE, VIBRATION AND ACTIVE CONTROL Pages 201 – 218

Observer-based Sliding Mode Control of Rijke-type Combustion Instability

Jaime Rubio-Hervas[1], Mahmut Reyhanoglu[2,*] and William MacKunis[2]
[1]*School of Mechanical and Aerospace Engineering, Nanyang Technological University, Singapore 639798, Singapore*
[2]*Physical Sciences Department, Embry-Riddle Aeronautical University, Daytona Beach, FL 32114, USA*

First submitted: 28 September 2014/Revised: 14 January 2015/Accepted: 18 January 2015

ABSTRACT

Observer-based sliding mode control of combustion instability in a Rijke-type thermoacoustic system is considered. A commonly used thermoacoustic model with sensors and monopole-like actuators is linearized and formulated in a state-space form. It is assumed that the velocity or pressure sensor locations are chosen to assure the observability of the system. An observer-based sliding mode controller is then implemented to tune the actuators so that the system is asymptotically stable. The effectiveness of the controller is illustrated through a simulation example involving two modes and one sensor. The successful demonstration indicates that the observer-based feedback controller can be applied to a real combustion system with multiple modes.

Keywords: Combustion instability, sliding modes, non-normality.

1. INTRODUCTION

Recently, researchers have given considerable attention to the control of thermoacoustic oscillations in Rijke-type combustion systems. Both passive and active control methods have been developed to prevent thermoacoustic instability, which is regarded as a major challenge for land-based gas turbine and aero-engine manufacturers [1-6]. Passive control [7] involves either applying acoustic dampers such as Helmholtz resonators [8, 9] and acoustic liners [10, 11] to increase the damping or redesigning the combustion system, such as changing the flame anchoring position or changing the operating conditions (see e.g., [7] and references therein). The passive approach is simple and requires low-cost maintenance. However, it cannot respond to changes in operating conditions. Therefore, it is desirable to use active control methods for the stabilization of the combustion systems.

Active controllers are essentially feedback controllers that drive the dynamic actuators in response to sensor measurements. There are two general actuation actions: modulating the acoustic field by using a monopole-like sound source such as a loudspeaker [12, 13], or modulating the unsteady heat release rate by using a secondary fuel injector [14-16]. An experimental study of using loudspeakers to dampen thermoacoustic instabilities was conducted by Campos-Delgado et al. [17] on a swirl-stabilized non-premixed spray combustor. The control was achieved by using a model-based controller such as linear quadratic Gaussian (LQG)/loop transfer recovery (LTR) and H^{∞} loop-shaping. Comparing the controllers' performance with that of a conventional phase-delay controller revealed that the model-based controllers resulted in larger reduction of the pressure oscillations.

* Corresponding author e-mail: reyhanom@erau.edu (M Reyhanoglu)

Detailed reviews of thermoacosutic instability and feedback control techniques can be found in the literature [18, 19]. The conventional linear controllers have focused on the unstable eigenmodes of the combustion system. Traditional linear controllers are designed to make the system stable by making the dominant eigenmodes decay exponentially. However, if the eigenmodes of the thermoacoustic system are non-orthogonal, controlling the dominant eigenmodes alone may cause other potential modes to become unstable due to the coupling between the acoustic modes [20]. Combustion systems have recently shown to be non-normal, characterized by non-orthogonal eigenmodes [21-23]. The non-orthogonality is found to be due to the presence of unsteady heat release or the complex impedance boundary conditions. It has also been found that in a linearly stable but non-normal system, there can be signicant transient growth of small perturbations before their eventual decay. If the transient growth is intense enough, combustion instability might be triggered. In order to prevent this, transient growth controllers have been proposed to achieve strict dissipativity [24-26].

In this work, a simplied Rijke-type thermoacoustic system with multiple actuators is considered. In Section 2, the dimensionless governing equations are described and the flow perturbations are expanded by using Galerkin series by following the work of Zhao and Li [27]. The model is linearized and formulated in state-space form. Section 3 introduces the design of a sliding mode controller. In Section 4, velocity and pressure measurements are introduced, and an observer design is proposed. A case study for two modes is presented, and its performance is evaluated in Section 5.

2. DESCRIPTION OF ACTUATED THERMOACOUSTIC MODEL

The thermoacoustic system examined in this paper, a horizontal Rijke tube with monopole-like actuators, is identical to that studied in [24-26, 28]. However, for completeness, a brief description of the actuated thermoacoustic model is reproduced.

2.1. Dimensionless governing equations

For convenience, the variables are non-dimensionalized as

$$u = \frac{\tilde{u}}{u_0}, \quad p = \frac{\tilde{p}}{\gamma M_0 p_0}, \quad \dot{Q}_s = \frac{\dot{\tilde{Q}}_s}{\gamma p_0 u_0},$$
$$x = \frac{\tilde{x}}{L_0}, \quad t = \frac{\tilde{t}c_0}{L_0}, \quad \frac{\delta(x - x_f)}{L_0} = \tilde{\delta}(\tilde{x} - \tilde{x}_f)$$

where the variables with tilde represent dimensional quantities; the quantity with a subscript 0 denotes the mean value; x denotes the dimensionless location along the duct (actuators and heat source are located at x_{ak} and x_f, respectively, as shown in Fig. 1), t denotes dimensionless time, M_0 is the mean Mach number, c_0 is the mean sound speed, L_0 is the length of the duct, and , γ is the ratio of specific heats.

The non-dimensional acoustic equations of such a thermoacoustic system in the presence of K actuators can then be written as

$$\frac{\partial u}{\partial t} + \frac{\partial p}{\partial x} = 0, \tag{1}$$

$$\frac{\partial p}{\partial t} + \varsigma p + \frac{\partial u}{\partial x} = (\gamma - 1)\dot{Q}_s \delta(x - x_f) + \gamma \sum_{k=1}^{K} \alpha_{ak} v_{ak} \delta(x - x_{ak}), \tag{2}$$

where ςp describes the thermo-viscous and friction damping across the heating element, and α_{ak} describes the ratio of the cross-sectional area S_{ak} of the kth actuator to the cross-sectional area S of the duct, i.e., $\alpha_{ak} = S_{ak}/S$. The non-dimensional heat release rate $\dot{Q}_s$ can be written as

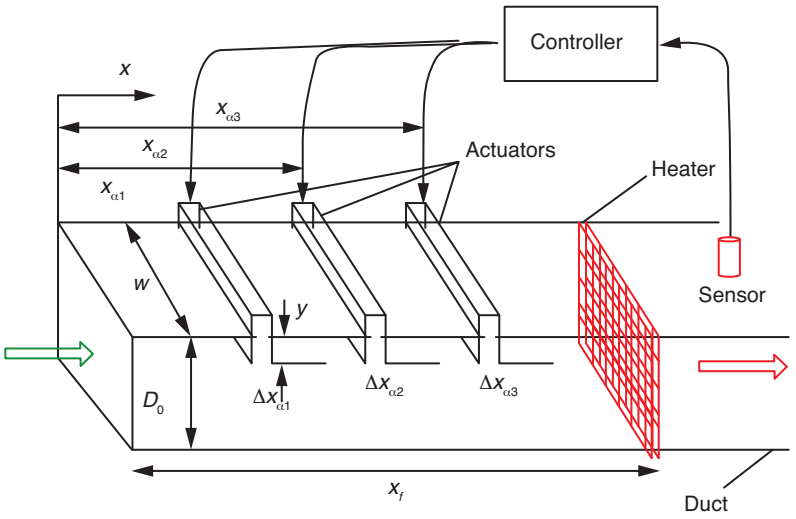

Figure 1: Diagram of a combustion system with monopole-like actuators modelled as movable pistons.

$$\dot{Q}_s = \kappa \left(\sqrt{\left| \frac{1}{3} + u_f(t-\tau) \right|} - \sqrt{\frac{1}{3}} \right), \tag{3}$$

with

$$\kappa = \frac{2L_w(T_w - \bar{T}_0)}{\sqrt{3u_0} S \gamma p_0} \sqrt{\pi \lambda c_v \rho_0 \frac{d_w}{2}}, \tag{4}$$

where d_w, L_w, and T_w denote the diameter, length and temperature of the heated wire, respectively; ρ denotes density, T temperature, λ and c_v are the thermal conductivity and specific heat at constant volume, respectively; and τ denotes the non-dimensional time delay describing the diference between the time when the oncoming velocity perturbation acts and the time when the corresponding heat release is felt. A subscript *ak* or *f* refers to the variable taken at the actuator or heat source location, respectively. The gas is assumed to be perfect, inviscid and non-heat conducting. The Mach number of the mean flow is assumed to be negligible and the heating element acoustically compact. It is also assumed that there is no mean temperature gradient.

The acoustic pressure p and velocity u inside the duct can be written as a superposition of the duct natural modes as

$$p(x,t) = -\sum_{j=1}^{N} \frac{\sin(j\pi x)}{j\pi} \dot{\eta}_j(t), \tag{5}$$

$$u(x,t) = \sum_{j=1}^{N} \cos(j\pi x) \eta_j(t), \tag{6}$$

where N represents the number of modes.

The actuation signal v_{ak} of the k^{th} monopole-like source such as a loud-speaker can now be expressed as

$$v_{ak}(t) = \mathcal{R}_k u(x_{ak}, t) + \mathcal{S}_k p(x_{ak}, t), \tag{7}$$

where $\mathcal{R}_k$ and $\mathcal{S}_k$ are dimensionless control parameters of the actuators. Discretizing the governing equations by substituting equations (5) and (6) into equation (2) and simplifying yields

$$\frac{\ddot{\eta}_j}{j\pi} + j\pi\eta_j + \varsigma_j \frac{\dot{\eta}_j}{j\pi} = -2(\gamma-1)\Big[\dot{Q}_s(x_f, t-\tau)\sin(j\pi x_f) + \frac{\gamma}{\gamma-1}\sum_{k=1}^{K}\alpha_{ak} v_{ak}(t)\sin(j\pi x_{ak})\Big]. \tag{8}$$

Note that in equation (8) the damping ς is taken into account by assigning a damping parameter ς_j to the jth mode. For the thermoacoustic system examined in this paper, p and $\frac{\partial u}{\partial x}$ are both set to zero at the ends of the duct (i.e., there is no acoustical energy being dissipated at the end boundaries). Furthermore, the acoustic waves are assumed to be planar such that there is also no acoustic energy being dissipated in the viscous and thermal boundary layers at the duct walls. Both types of dissipations are modelled by the damping parameter for each mode

$$\varsigma_j = c_1 j^2 + c_2 j^{1/2}, \tag{9}$$

where c_1 and c_2 are to be the same for each mode. This dissipation model has been widely used [21, 26]. The actuated nonlinear thermoacoustic model as described in this paper contains the most influential characteristics as discussed in more sophisticated flame-involved control models.

2.2. Linearization of the governing equations

Define

$$\mathbf{x} = [\eta_1, \eta_2, \cdots, \eta_N]^T, \quad \dot{\mathbf{x}} = [\dot{\eta}_1, \dot{\eta}_2, \cdots, \dot{\eta}_N]^T,$$
$$\boldsymbol{\psi} = [\cos(\pi x), \cos(2\pi x), \cdots, \cos(N\pi x)]^N,$$
$$\boldsymbol{\phi} = \left[\frac{\sin(\pi x)}{\pi}, \frac{\sin(2\pi x)}{2\pi}, \cdots, \frac{\sin(N\pi x)}{N\pi}\right]^N,$$
$$\mathbf{M} = \mathrm{diag}\left\{\frac{1}{\pi}, \frac{1}{2\pi}, \cdots, \frac{1}{N\pi}\right\}, \quad \mathbf{D}_d = \mathrm{diag}\left\{\frac{\varsigma_1}{\pi}, \frac{\varsigma_2}{2\pi}, \cdots, \frac{\varsigma_N}{N\pi}\right\},$$

and denote by $\boldsymbol{\chi} = [\boldsymbol{\chi}_1^T, \boldsymbol{\chi}_2^T]^T$ the state vector, where $\boldsymbol{\chi}_1 = \mathbf{x}$ and $\boldsymbol{\chi}_1 = \mathbf{M}\dot{\mathbf{x}}$. Then, it has been shown by Zhao and Reyhanoglu [24] that, for a control input

$$\mathbf{u} = -2\gamma\left(\sum_{k=1}^{K}\alpha_{ak}\mathcal{R}_k\mathbf{M}^{-1}\boldsymbol{\phi}_{ak}\boldsymbol{\psi}_{ak}^T\right)\mathbf{x} + 2\gamma\left(\sum_{k=1}^{K}\alpha_{ak}\mathcal{S}_k\mathbf{M}^{-1}\boldsymbol{\phi}_{ak}\boldsymbol{\phi}_{ak}^T\right)\dot{\mathbf{x}}, \tag{10}$$

the linearized state space equations can be written as

$$\dot{\boldsymbol{\chi}} = \mathbf{A}\boldsymbol{\chi} + \mathbf{B}\mathbf{u}, \tag{11}$$

where

$$\mathbf{A} = \begin{bmatrix} \mathbf{0} & \mathbf{M}^{-1} \\ \mathbf{A}_1 & \mathbf{A}_2 \end{bmatrix}, \quad \mathbf{B} = \begin{bmatrix} \mathbf{0} \\ \mathbf{I} \end{bmatrix}, \tag{12}$$

and

$$\mathbf{A}_1 = -\left(\mathbf{M}^{-1} + (\gamma-1)\sqrt{3}\,\kappa\mathbf{M}^{-1}\boldsymbol{\phi}_f\boldsymbol{\psi}_f^T\right),$$
$$\mathbf{A}_2 = -\left(\mathbf{D}_d - (\gamma-1)\sqrt{3}\,\kappa\tau\mathbf{M}^{-1}\boldsymbol{\phi}_f\boldsymbol{\psi}_f^T\right)\mathbf{M}^{-1}.$$

2.3. Definition of transient acoustical energy growth

To characterize the transient growth of flow disturbances, it is necessary to define a measure in the system. The total acoustical energy E(t) per unit cross-sectional area is chosen as the measure which is defined in terms of dimensionless variables as

$$E(t) = \frac{1}{2}\int_0^1 \left(p^2(x,t) + u^2(x,t)\right) \mathrm{d}x = \left(\frac{1}{2}\right)^2 \sum_{j=1}^{N} \left[\eta_j^2 + \left(\frac{\dot{\eta}_j}{j\pi}\right)^2\right] = \left(\frac{1}{2}\right)^2 \|\chi\|^2. \quad (13)$$

The acoustical transient energy growth is then defined as the ratio of acoustical energy at some instant of time to the initial energy level, i.e.,

$$G(t) = \max_{E(0)} \frac{E(t)}{E(0)}. \quad (14)$$

When $G_{\max} = \max_t G(t) > 1$, then the acoustical energy is increased for some time t (known as transient growth). When $G_{\max} = 1$, there is no transient growth of the acoustical energy. In other words, the rate of acoustical energy change at any instant of time is non-positive in the sense that

$$\frac{dE}{dt} \leq 0 \quad (15)$$

for all initial conditions.

In the following analysis, the system considered is associated with only 2 modes (i.e., $N = 2$). Note that this analysis can be easily extended to systems with a given N number of modes.

3. DESIGN OF A SLIDING MODE CONTROLLER

Consider a sliding mode controller of the form

$$\mathbf{u} = -\mathbf{K}\mathrm{sign}(\mathbf{S}(\chi)) \quad (16)$$

where $\mathbf{S}(\chi)$ represents the switching function

$$\mathbf{S}(\chi) = [s_1(\chi), s_1(\chi)]^T = \chi_2 + \mathbf{\Lambda}\chi_1 \quad (17)$$

and $\mathbf{\Lambda} = \mathrm{diag}\{\lambda_1, \lambda_2\}$, $\lambda_i > 0$, $i = 1, 2$. Note that here $\mathrm{sign}(\mathbf{S}(\chi)) = [\mathrm{sign}(s_1(\chi)), \mathrm{sign}(s_2(\chi))]^T$.

By choosing a Lyapunov function

$$V = \frac{1}{2}\mathbf{S}^T(\chi)\mathbf{S}(\chi), \quad (18)$$

and noting that the derivative of the switching function in equation (17) along the trajectories of equation (11) yields

$$\dot{\mathbf{S}}(\chi) = \dot{\chi}_2 + \Lambda\chi_1 = \mathbf{A}_1\chi_1 + (\mathbf{A}_2 + \mathbf{\Lambda}\mathbf{M}^{-1})\chi_2 + \mathbf{u}, \quad (19)$$

the derivative of the Lyapunov function for the control input in equation (16) can be expressed as

$$\dot{V} = \mathbf{S}^T(\chi)\left[\mathbf{N}(\chi) - \mathbf{K}\mathrm{sign}(\chi)\right], \quad (20)$$

where $\mathbf{N}(\chi) = \mathbf{A}_1\chi_1 + (\mathbf{A}_2 + \mathbf{\Lambda}\mathbf{M}^{-1})\chi_2$. Defining now $\mathbf{K} = \mathrm{diag}\{K_1, K_2\}$, $K_i > 0$, $i = 1, 2$, such that

$$K_i > |N_i|, i = 1,2, \tag{21}$$

sliding mode existence on the manifold $\{\boldsymbol{\chi}:\mathbf{S}(\boldsymbol{\chi}) = \mathbf{0}\}$ is clearly guaranteed such that once the state reaches the manifold $\mathbf{S} = \boldsymbol{\chi}_2 + \boldsymbol{\Lambda}\boldsymbol{\chi}_1 = 0 \Rightarrow \dot{\boldsymbol{\chi}}_1 = -\mathbf{M}^{-1}\boldsymbol{\Lambda}\boldsymbol{\chi}_1$, and therefore $\boldsymbol{\chi}_1 \to \mathbf{0}$ as $t \to \infty$.

Note that the following approximation can be made:

$$\text{sign}(\mathbf{S}(\boldsymbol{\chi})) \approx \begin{bmatrix} \dfrac{s_1(\boldsymbol{\chi})}{|s_1(\boldsymbol{\chi})| + \delta_1} \\ \dfrac{s_2(\boldsymbol{\chi})}{|s_2(\boldsymbol{\chi})| + \delta_2} \end{bmatrix}, \tag{22}$$

where δ_1 and δ_2 are small parameters, such that the control input $\mathbf{u}$ can be rewritten as

$$\mathbf{u} = -\mathbf{M}_1\boldsymbol{\chi}_1 - \mathbf{M}_2\boldsymbol{\chi}_2, \tag{23}$$

where

$$\mathbf{M}_1 = \begin{bmatrix} \dfrac{K_1\lambda_1}{|s_1(\boldsymbol{\chi})| + \delta_1} & 0 \\ 0 & \dfrac{K_2\lambda_2}{|s_2(\boldsymbol{\chi})| + \delta_2} \end{bmatrix}, \quad \mathbf{M}_1 = \begin{bmatrix} \dfrac{K_1}{|s_1(\boldsymbol{\chi})| + \delta_1} & 0 \\ 0 & \dfrac{K_2}{|s_2(\boldsymbol{\chi})| + \delta_2} \end{bmatrix}.$$

The controller can now be realized using the dimensionless controller parameters $\mathcal{R}_k$ and $\mathcal{S}_k$ by choosing

$$\mathbf{M}_1 = 2\gamma\sum_{k=1}^{K}\alpha_{ak}\mathcal{R}_k\mathbf{M}^{-1}\boldsymbol{\phi}_{ak}\boldsymbol{\psi}_{ak}^T, \tag{24}$$

$$\mathbf{M}_2 = -2\gamma\sum_{k=1}^{K}\alpha_{ak}\mathcal{S}_k\mathbf{M}^{-1}\boldsymbol{\phi}_{ak}\boldsymbol{\phi}_{ak}^T\mathbf{M}^{-1}. \tag{25}$$

4. OBSERVER-CONTROLLER DESIGN

In a practical thermoacoustic system, velocity and pressure sensors are used for experimental measurements. It is shown later that, in the presence of one of the velocity or pressure sensors, the thermoacoustic system is observable. Therefore, the state vector can be estimated. Moreover, such observable systems are exposed to perturbations in the dynamic model as well as in the sensors measurements. A sliding mode observer allows estimation of the state in a robust way and presents some advantages with respect to the classical linear observers in case of noisy measurements, especially in the situation when noise information is not exactly known.

Introducing sensors which can only measure the velocity or pressure values at M diferent locations x_{sl}, $l = 1,\ldots, M$, respectively; the linearized system in equation (11) can be rewritten as

$$\dot{\boldsymbol{\chi}} = \mathbf{A}\boldsymbol{\chi} + \mathbf{B}\mathbf{u} + \mathbf{v}, \tag{26}$$

$$\mathbf{y} = \mathbf{C}\boldsymbol{\chi} + \mathbf{w} \tag{27}$$

where $\mathbf{y}$ is the measured output and $\mathbf{v}$,$\mathbf{w}$ denote the process and observer noises, respectively.

If velocity sensors are used, then $\mathbf{y} = [u(x_{s1}, t), u(x_{s2}, t),\ldots, u(x_{sM}, t)]^T$ and the following output matrix can be obtained

$$\mathbf{C} = \begin{bmatrix} \boldsymbol{\psi}_S^T & \mathbf{0} \end{bmatrix}, \tag{28}$$

where

$$\boldsymbol{\psi}_S = \begin{bmatrix} \psi_{s1} & \psi_{s1} & \cdots & \psi_{sM} \end{bmatrix}.$$

On the other hand, for pressure sensors $\mathbf{y} = [p(x_{s1}, t), p(x_{s2}, t),\ldots, p(x_{sM}, t)]^T$ and the output matrix has the following form:

$$\mathbf{C} = \begin{bmatrix} \mathbf{0} & -\boldsymbol{\phi}_S^T \mathbf{M}^{-1} \end{bmatrix}, \tag{29}$$

where

$$\boldsymbol{\phi}_S = \begin{bmatrix} \boldsymbol{\phi}_{s1} & \boldsymbol{\phi}_{s1} & \cdots & \boldsymbol{\phi}_{sM} \end{bmatrix}.$$

In both cases, sensor locations can be chosen such that the system is observable, i.e.,

$$\text{rank}\left[\mathbf{C}^T \mathbf{A}^T \boldsymbol{C}^T \cdots (\mathbf{A}^T)^3 \mathbf{C}^T\right] = 4.$$

For a sliding operator given by a "sign" function, the sliding mode observer equation takes the form

$$\dot{\hat{\boldsymbol{\chi}}} = \mathbf{A}\hat{\boldsymbol{\chi}} + \mathbf{B}\mathbf{u} + \mathbf{L}\text{sign}(\mathbf{y} - \mathbf{C}\hat{\boldsymbol{\chi}}), \tag{30}$$

where $\hat{\boldsymbol{\chi}}$ denotes the estimated state based on the measurements of $\mathbf{y}$, and $\mathbf{L}$ is a gain matrix.

In this paper, for simplicity in presenting the ideas, it is assumed that a single velocity or pressure sensor is available (i.e., $M = 1$). The development in the paper can easily be extended for the more general case.

4.1. Velocity sensor

Assume that a velocity sensor is available and located at $x_s = 0.25$ such that

$$\mathbf{C} = \begin{bmatrix} 1/\sqrt{2}, 0, 0, 0 \end{bmatrix},$$

and define $\xi_1 = \eta_1$ and $\boldsymbol{\xi}_2 = [\eta_2, \dot{\eta}_1/\pi, \dot{\eta}_2/2\pi]^T$ so that the state vector can be now partitioned as $\boldsymbol{\chi} = [\xi_1, \boldsymbol{\xi}_2^T]^T$. Then, combining equations (11) and (30), the observation error dynamics (i.e., $\bar{\boldsymbol{\chi}} = \boldsymbol{\chi} - \hat{\boldsymbol{\chi}}$) can be written as

$$\dot{\bar{\xi}}_1 = \mathbf{A}'_{12}\bar{\boldsymbol{\xi}}_2 - L_1 \text{sign}(\bar{\xi}_1), \tag{31}$$

$$\dot{\bar{\boldsymbol{\xi}}}_2 = \mathbf{A}_{21}\bar{\xi}_1 + \mathbf{A}_{22}\bar{\boldsymbol{\xi}}_2 - \mathbf{L}_2 \text{sign}(\bar{\xi}_1), \tag{32}$$

where $\mathbf{A}'_{12}, \mathbf{A}'_{21}$ and $\mathbf{A}'_{22}$ are partitions of the matrix $\mathbf{A}$ and their expressions can be found in the Appendix. From equation (31), it follows that sliding mode exists in an area such that $L_1 > |\mathbf{A}'_{21}\bar{\boldsymbol{\xi}}_2|$ When sliding starts $\dot{\bar{\xi}}_1 = 0$ and the equivalent value of the switching function is $\{L_1 \text{sign}(\bar{\xi}_1)\}_{\text{eq}} = \mathbf{A}'_{12}\bar{\boldsymbol{\xi}}_2$, i.e., the system in sliding mode is described by the equation

$$\dot{\bar{\boldsymbol{\xi}}}_2 = \left(\mathbf{A}'_{22} - \frac{1}{L_1}\mathbf{L}_2\mathbf{A}'_{12}\right)\bar{\boldsymbol{\xi}}_2. \tag{33}$$

From this equation it follows that the observer gain $\mathbf{L}_2$ can be chosen such that the eigenvalues of the matrix $\mathbf{A}'_{22} - \frac{1}{L_1}\mathbf{L}_2\mathbf{A}'_{12}$ have negative real parts.

4.2. Pressure sensor

Assume now that a pressure sensor is located at $x_s = 0.5$ such that

$$\mathbf{C} = [0, 0, -1/\pi, 0],$$

and define $\xi_1 = \dot{\eta}_1/\pi$ and $\boldsymbol{\xi}_2 = [\eta_1, \eta_2, \dot{\eta}_2/2\pi]^T$. Then, the observation error dynamics can be written as

$$\dot{\bar{\xi}}_1 = a_{11}\bar{\xi}_1 + \mathbf{A}_{12}\bar{\boldsymbol{\xi}}_2 + L_1 \text{sign}(\bar{\xi}_1), \tag{34}$$

$$\dot{\bar{\boldsymbol{\xi}}}_2 = \mathbf{A}_{21}\bar{\xi}_1 + \mathbf{A}_{22}\bar{\boldsymbol{\xi}}_2 + \mathbf{L}_2 \text{sign}(\bar{\xi}_1), \tag{35}$$

where the expressions of the above matrices can be found in the Appendix. Similarly, from equation (34) it follows that sliding mode exists in an area such that $L_1 < -|\boldsymbol{a}'_{11}\bar{\xi}_1 + \boldsymbol{A}'_{12}\bar{\boldsymbol{\xi}}_2|$ When sliding starts $\bar{\xi}_1 = 0$ and the equivalent value of the switching function is $\{L_1 \text{sign}(\bar{\xi}_1)\}_{\text{eq}} = -\mathbf{A}'_{12}\bar{\boldsymbol{\xi}}_2$, i.e., the system in sliding mode is described by the equation

$$\dot{\bar{\boldsymbol{\xi}}}_2 = \left(\mathbf{A}'_{22} - \frac{1}{L_1}\mathbf{L}_2\mathbf{A}'_{12}\right)\bar{\boldsymbol{\xi}}_2. \tag{36}$$

Again, the observer gain $\mathbf{L}_2$ can be chosen such that the eigenvalues of the matrix $\mathbf{A}'_{22} - \frac{1}{L_1}\mathbf{L}_2\mathbf{A}'_{12}$ have negative real parts.

5. SIMULATIONS

The feedback control law developed in the previous section is implemented on a system with two modes. The actuators locations are chosen at $x_{a1} = 0.3$, $x_{a2} = 0.35$, $x_{a3} = 0.45$, and $x_{a4} = 0.55$. The physical parameters used in the simulations are given in Table 1. Initial conditions at the heat source location are $p(x_f, 0) = 0$ and $u(xf, 0) = -0.1675$ for $x_f = 0.7$.

The sliding mode controller is implemented as in equation (16) by choosing

$$\boldsymbol{\Lambda} = \begin{bmatrix} 0.1 & 0 \\ 0 & 0.1 \end{bmatrix}, \quad \mathbf{K} = \begin{bmatrix} 1 & 0 \\ 0 & 1 \end{bmatrix}\left(|N_1(\hat{\boldsymbol{\chi}})| + |N_2(\hat{\boldsymbol{\chi}})|\right),$$

and $\delta_1 = \delta_2 = 0.1$. This controller is applied to the actual nonlinear system.

Table I.
Parameters.

Parameter	Value	Parameter	Value
ρ	1.025 kg/m^3	λ	0.0328 W/m.K
c_v	719 J/kg.K	γ	1.4
L_0	1 m	L_w	2.5 m
c_0	344 m/s	u_0	0.3 m/s
T_0	295 K	T_w	1680 K
d_w	0.5 x 10^{-3} m	S	1.56 x 10^{-3} m^2
P_0	8.69 x 10^4 Pa	τ	0.04 (0.1 ms)
ς_1	0.0440	ς_2	0.1657
α_{a1}	0.01	α_{a2}	0.01

In the presence of velocity sensors, the observer gain is first defined by $L_1 = 2$. Then, the following eigenvalues of $\mathbf{A}'_{22}-\mathbf{L}_2\mathbf{A}'_{12}/L_1$ are assigned:

$$(-0.1 \pm 6.5i, -3)$$

such that $\mathbf{L}_2$ =[-2.65, 1.94, -1.98]^T and, thus, the matrix $\mathbf{L}$ can be written as $\mathbf{L} = [2, -2.65, 1.94, -1.98]^T$. Similarly, in the presence of pressure sensors, the matrix $\mathbf{L}$ is defined as $\mathbf{L} = [3.32, -1.82, -2, 1.33]^T$ which results in the same eigenvalues for $\mathbf{A}'_{22}-\mathbf{L}_2\mathbf{A}'_{12}/L_1$.

Noise has been introduced using the "Random Number" block in Simulink which outputs a normally (Gaussian) distributed random signal. Zero mean and 1×10^{-4} variance have been assumed for the observation noises. Figure 2 first shows that, in the absence of any control input the system is linearly unstable. Then as the above controller is implemented, the nondimensionalized velocity and pressure perturbations at the heat source location converge as it is shown in Figures 3 and 4.

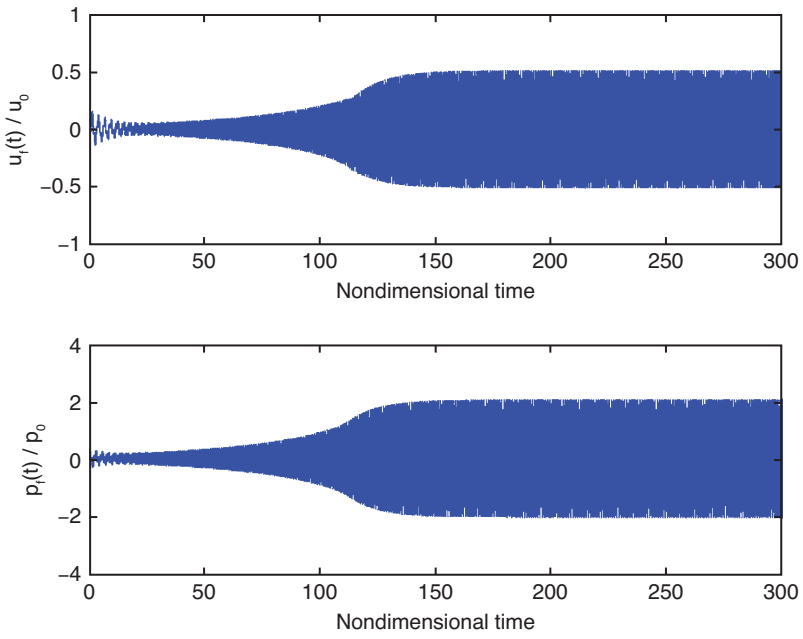

Figure 2: Time responses of velocity *u* and pressure *p* at the heat source location (zero input case).

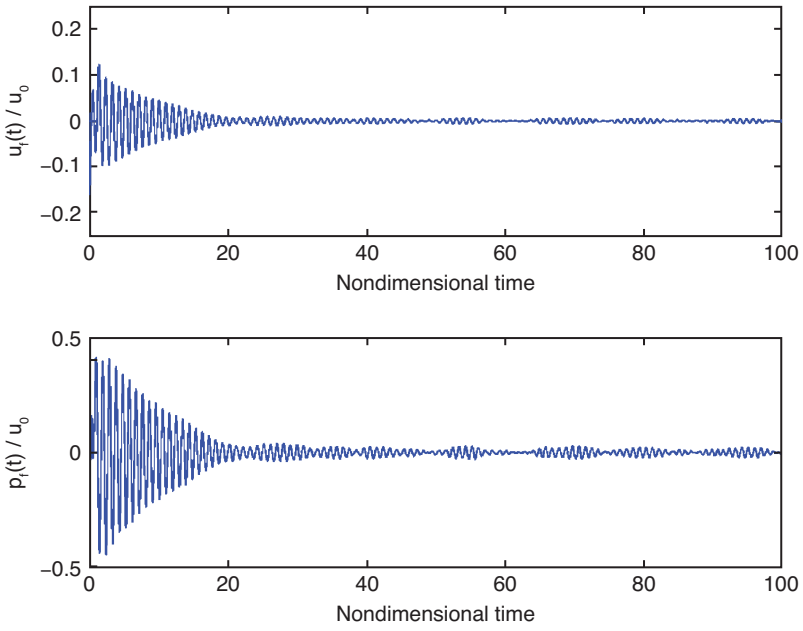

Figure 3: Time responses of velocity *u* and pressure *p* at the heat source location (velocity sensor).

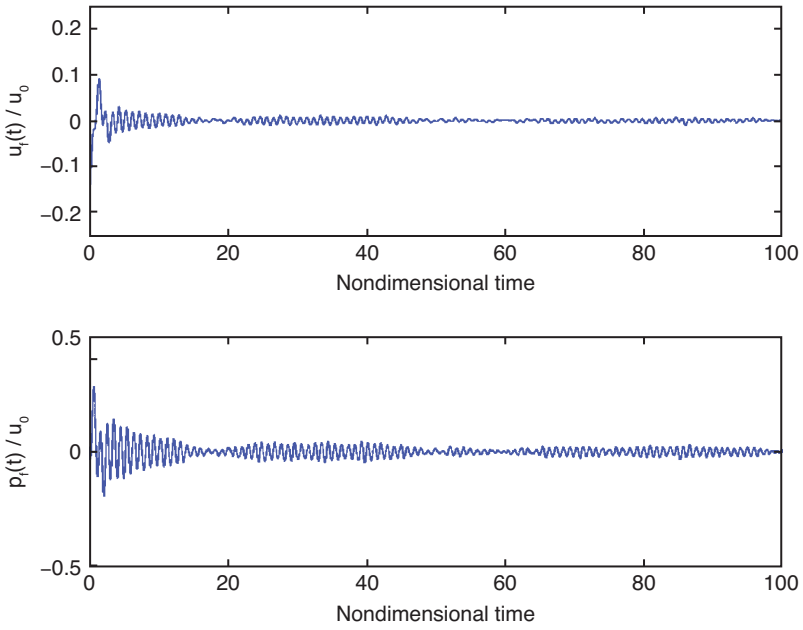

Figure 4: Time responses of velocity *u* and pressure *p* at the heat source location (pressure sensor).

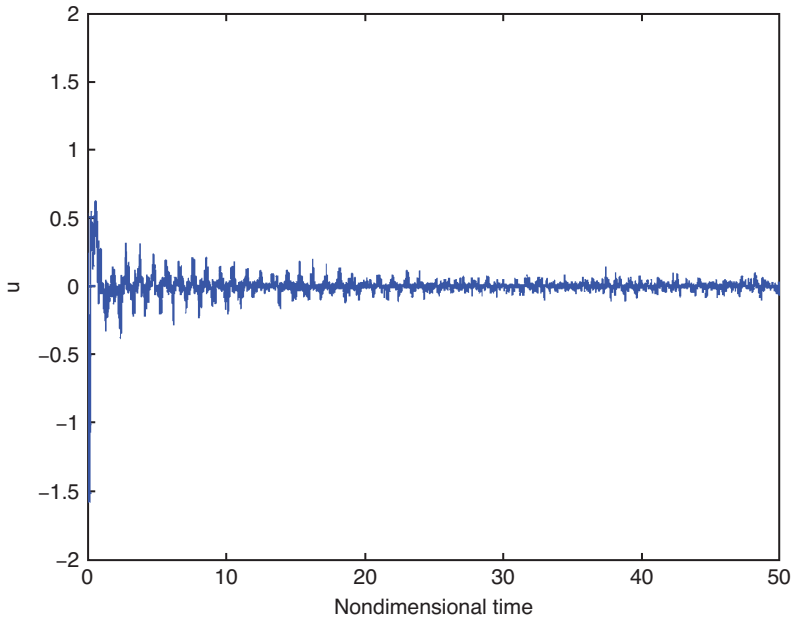

Figure 5: Time response of control input **u** (velocity sensor).

Figures 5 and 6 show the control effort. The related control parameters $\mathcal{R}_k$ and $\mathcal{S}_k$ are represented in Figures 7-10. The estimation errors are illustrated in Figures 11 and 12. Figures 13 and 14 illustrate the existence of transient growth of the acoustical energy. It can be seen that similar results are expected from using either velocity or pressure sensors, both in terms of the time response and effort control.

6. CONCLUSION

In this work, observer-based feedback control of combustion instability in a Rijke-type thermoacoustic system has been considered. A generalized thermoacoustic model with monopole-like actuators is used and combined with a sliding mode controller, which is designed especially for this work. It has been shown that in the presence of either velocity or pressure sensors, the system is

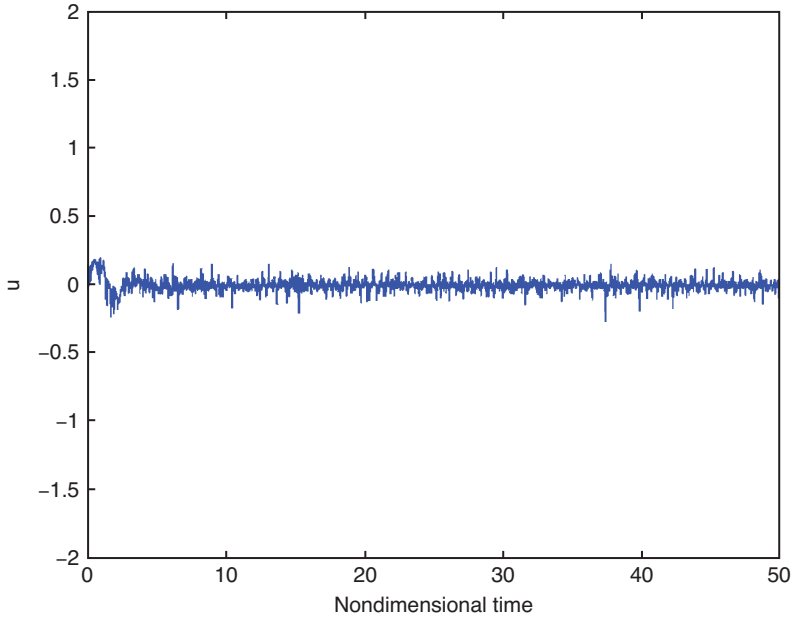

Figure 6: Time response of control input **u** (pressure sensor).

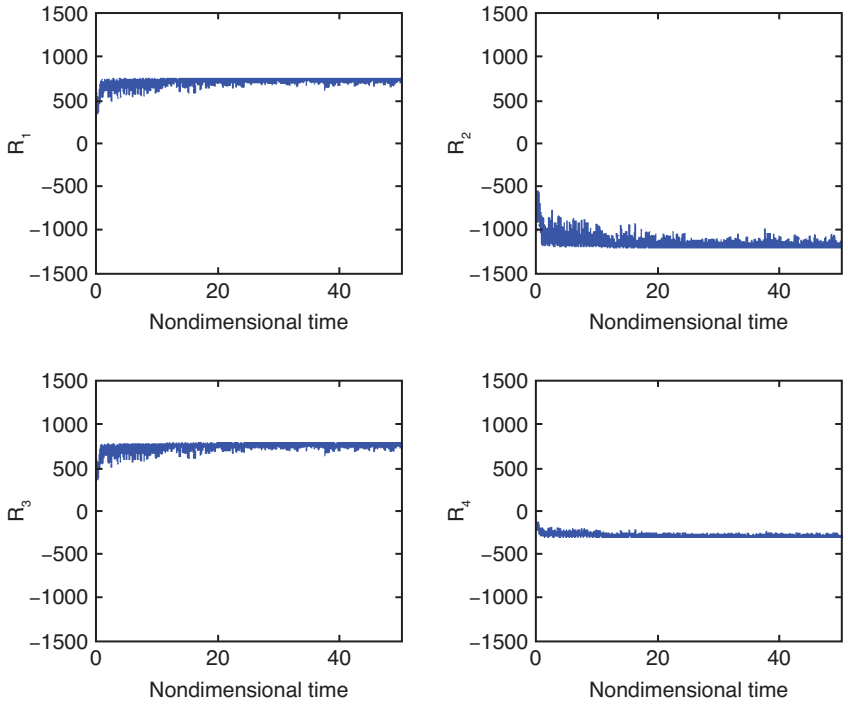

Figure 7: Time response of control parameters $\mathcal{R}_k$ (velocity sensor).

observable, and subsequently, an observer design has been introduced. As the observer-based controller is implemented to tune the actuators, the system becomes asymptotically stable. The performance of the controller is illustrated with a system involving two modes. Future work includes extensions to cope with the nonlinear dynamics of the combustion system as well as generalizing the concepts above to any number of modes and sensors.

ACKNOWLEDGEMENTS

The authors wish to acknowledge the support provided by Nanyang Technological University.

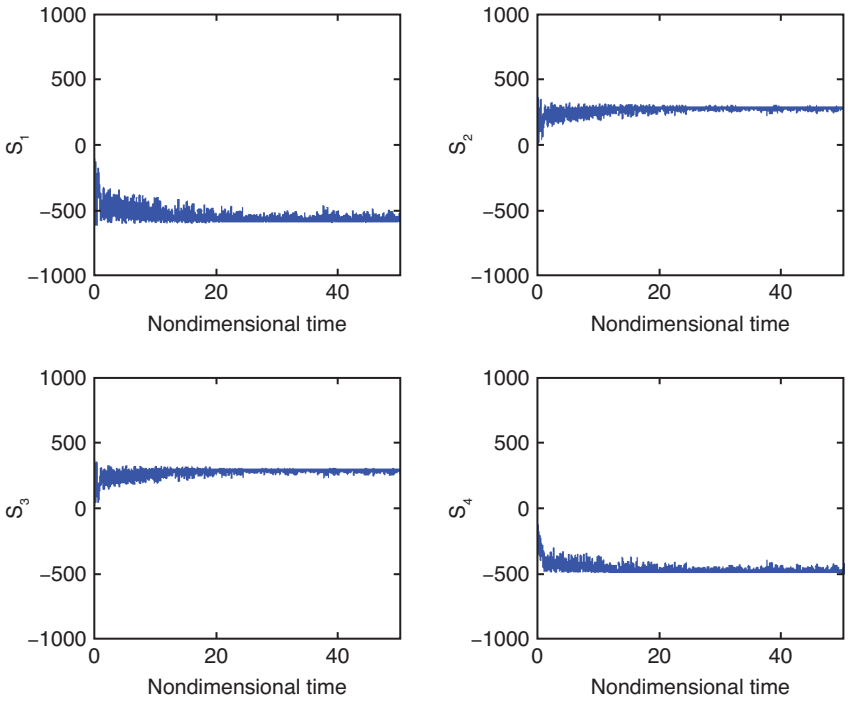

Figure 8: Time response of control parameters $\mathcal{S}_k$ (velocity sensor).

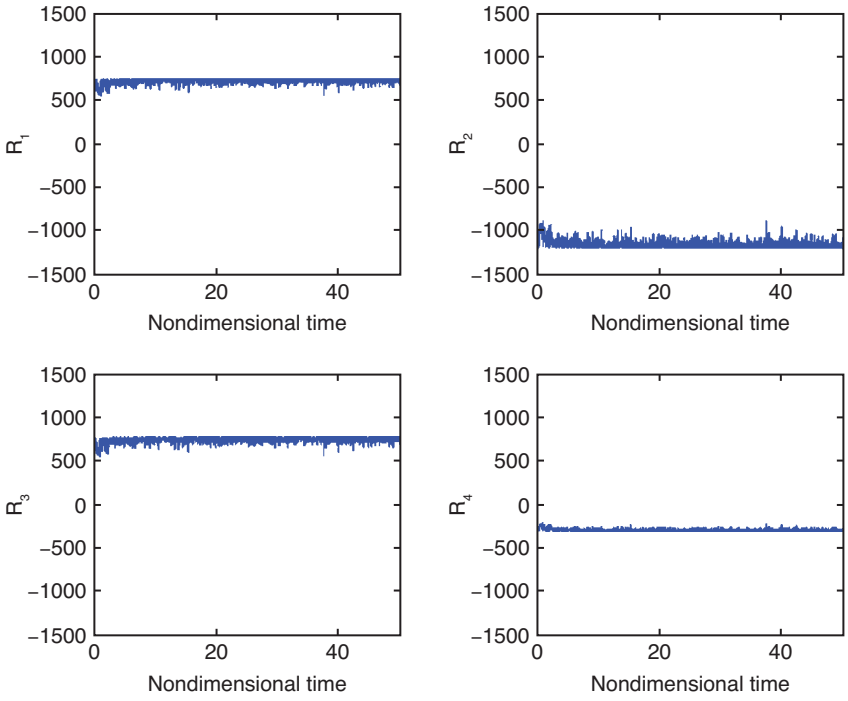

Figure 9: Time response of control parameters $\mathcal{R}_k$ (pressure sensor).

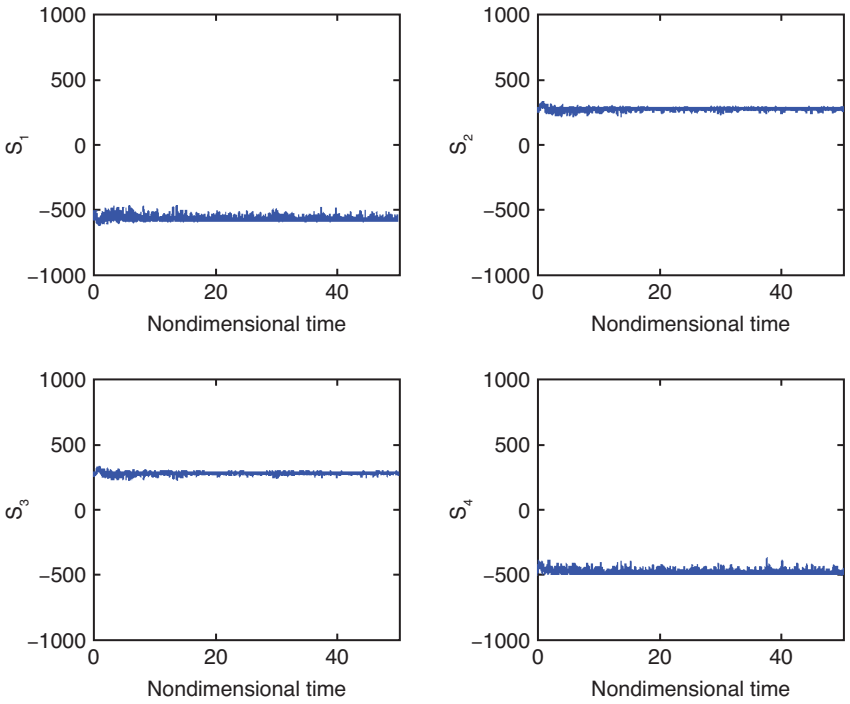

Figure 10: Time response of control parameters S_k (pressure sensor).

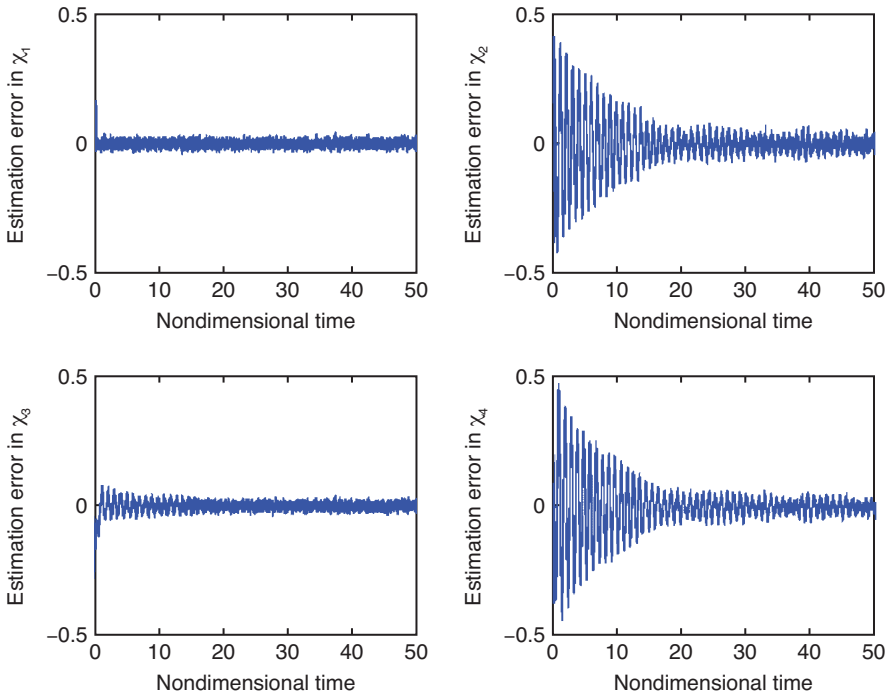

Figure 11: Time response of estimation errors $\tilde{\chi}$ (velocity sensor).

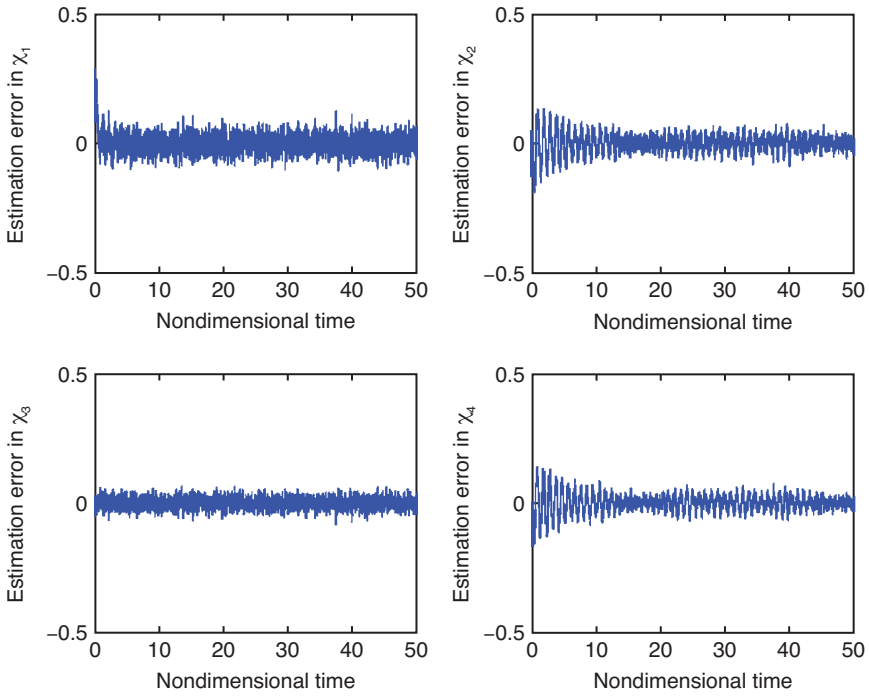

Figure 12: Time response of estimation errors $\tilde{\chi}$ (pressure sensor).

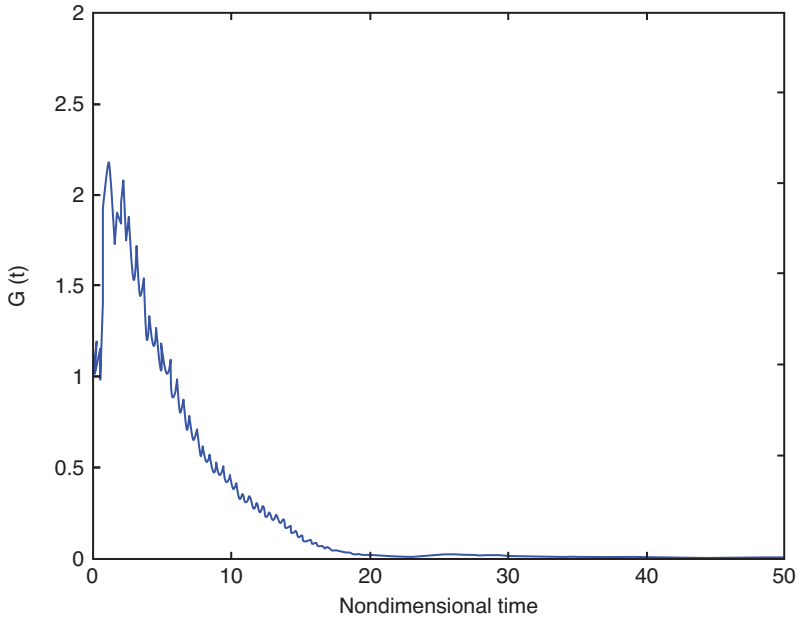

Figure 13: Flow disturbance transient energy growth rate (velocity sensor).

APPENDIX

Matrix **A** in equation (11) can be particularized for $N = 2$ modes as:

$$\mathbf{A} = \begin{bmatrix} 0 & 0 & \pi & 0 \\ 0 & 0 & 0 & 2\pi \\ A_{11} & A_{12} & A_{13} & A_{14} \\ A_{21} & A_{22} & A_{23} & A_{24} \end{bmatrix}$$

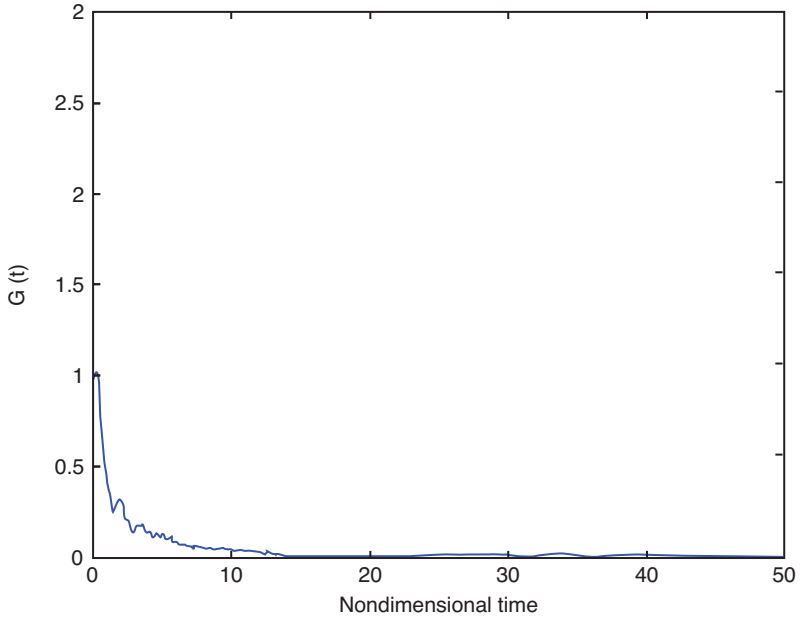

Figure 14: Flow disturbance transient energy growth rate (pressure sensor).

where

$$A_{11} = -\pi - (\gamma - 1)\sqrt{3}\kappa \sin(\pi x_f)\cos(\pi x_f),$$
$$A_{12} = -(\gamma - 1)\sqrt{3}\kappa \sin(\pi x_f)\cos(2\pi x_f),$$
$$A_{13} = -\varsigma_1 + (\gamma - 1)\sqrt{3}\kappa\tau\pi \sin(\pi x_f)\cos(\pi x_f),$$
$$A_{14} = (\gamma - 1)\sqrt{3}\kappa\tau 2\pi \sin(\pi x_f)\cos(2\pi x_f),$$
$$A_{21} = -(\gamma - 1)\sqrt{3}\kappa \sin(2\pi x_f)\cos(\pi x_f),$$
$$A_{22} = -2\pi - (\gamma - 1)\sqrt{3}\kappa \sin(2\pi x_f)\cos(2\pi x_f),$$
$$A_{23} = (\gamma - 1)\sqrt{3}\kappa\tau\pi \sin(2\pi x_f)\cos(\pi x_f),$$
$$A_{24} = -\varsigma_2 + (\gamma - 1)\sqrt{3}\kappa\tau 2\pi \sin(2\pi x_f)\cos(2\pi x_f).$$

Then it can be easily shown that, in the presence of velocity sensors, the partitions used in the previous sections are given by:

$$\mathbf{A}_{12}^{'} = \begin{bmatrix} 0 & \pi & 0 \end{bmatrix}, \quad \mathbf{A}_{21}^{'} = \begin{bmatrix} 0 \\ A_{11} \\ A_{21} \end{bmatrix}, \quad \mathbf{A}_{22}^{'} = \begin{bmatrix} 0 & 0 & 2\pi \\ A_{12} & A_{13} & A_{14} \\ A_{22} & A_{23} & A_{24} \end{bmatrix},$$

whereas for pressure sensors:

$$a_{11}^{'} = A_{13}, \quad \mathbf{A}_{12}^{'} = \begin{bmatrix} A_{11} & A_{12} & A_{13} \end{bmatrix}, \quad \mathbf{A}_{12}^{'} = \begin{bmatrix} \pi \\ 0 \\ A_{23} \end{bmatrix}, \quad \mathbf{A}_{22}^{'} = \begin{bmatrix} 0 & 0 & 0 \\ 0 & 0 & 2\pi \\ A_{21} & A_{22} & A_{24} \end{bmatrix}.$$

REFERENCES

[1] Langhorne PJ, Reheat buzz: an Acoustically coupled combustion instability-Part 1: Experiment. Journal of Fluid Mechanics (1988), 193, 417-443.

[2] Yang V and Anderson WE, Liquid Rocket Engine Combustion Instabilities (1995), AIAA Inc, USA.

[3] Dowling AP, A kinematic model of a ducted flame. Journal of Fluid Mechanics (1999), 394, 51-72.

[4] Lieuwen TC and Yang V, Combustion Instabilities in Gas Turbine Engines: Operational Experience, Fundamental Mechanisms and Modeling (2005), AIAA Inc, USA.

[5] Palies P, Durox D, Schuller T and Candel S, Nonlinear combustion instability analysis based on flame describing function applied to turbulent premixed swirling flames, Combustion and Flame (2011), 158(1), 1980-1991.

[6] Kim KT and Hochgreb S, Measurements of triggering and transient growth in a model lean-premixed gas turbine combustor. Combustion and Flame (2012), 159, 1215-1227.

[7] Richards GA, Straub DL and Robey EH, Passive control of combustion dynamics in stationary gas turbines. Journal of Propulsion and Power (2003), 19(5), 795-810.

[8] Gysling DL, Copeland GS, McCormick DC and Proscia WM, Combustion system damping augmentation with helmholtz resonator. Journal of Engineering for Gas Turbines and Power (2000), 122(1), 269-274.

[9] Zhao D and Morgans AS, Tuned passive control of combustion instabilities using multiple Helmholtz resonators. Journal of Sound and Vibration (2009), 320(4-5), 744-757.

[10] Eldredge JD and Dowling AP, The absorption of axial acoustic wave by a perforated liner with bias flow. Journal of Fluid Mechanics (2003), 485(1), 307-335.

[11] Zhong Z and Zhao D, Time-domain characterizaton of the acoustic damping of a perforated liner with bias flow. Journal of the Acoustical Society of America (2011), 132(1), 271-282.

[12] Heckl MA, Active control of the noise from a Rijke tube. Journal of Sound and Vibration (1984), 124(1), 117-133.

[13] Zhao D and Chow ZH, Thermoacoustic instability of a laminar premixed flame in Rijke tube with a hydrodynamic region. Journal of Sound and Vibration (2013), 332, 3419–3437.

[14] Seume JR, Vortmeyer N, Krause W, Hermann J, Hantschk CC, Zangl P, Gleis S and Vortmeyer D, Application of active combustion instability control to a heavy duty gas turbine. Journal of Engineering for Gas Turbines and Power (1998), 120(1), 721-726.

[15] Sattinger SS, Neumeier Y, Nabi A, Zinn BT, Amos DJ and Darling DD, Subscale demonstration of the active feedback control of gas turbine combustion instability, Transactions of the ASME (2000), 262(1), 262-268.

[16] Bernier D, Ducruix S, Lacas F, Candel S, Robart N and Poinsot T, Transfer function measurments in a model combustor: application to adaptive instability control, Combustion Science and Technology (2003), 175(6), 993-1015.

[17] Campos-Delgado DU, Zhou K, Allgood D and Acharya S, Active control of combustion instabilities using model-based controllers. Combustion Science and Technology (2003), 175(1), 27-53.

[18] McManus KR, Poinsot T and Candel SM, A review of active control of combustion instabilities. Progress in Energy and Combustion Science, 1993, 19, 1-29.

[19] Dowling AP and Morgans AS, Feedback control of combustion oscillations, Annual Review of Fluid Mechanics (2005), 37, 151-182.

[20] Annaswamy AM, Fleifil M, Hathout JP and Ghoniem AF, Impact of linear coupling on the design of active controllers for thermoacoustic instability, Combustion Science and Technology (1997), 128(1), 131-180.

[21] Juniper MP, Triggering in the horizontal Rijke tube: Non-normality, transient growth and by-pass transition. Journal of Fluid Mechanics (2011), 667, 272-308.

[22] Wieczorek K, Sensiau C, Polifke W and Nicoud F, Assessing non-normal effects in thermoacoustic systems with mean flow. Physics of Fluids (2011), 23, 107-103.

[23] Zhao D, Transient growth of flow disturbances in triggering a Rijke tube combustion instability. Combustion and Flame (2012), 256(1), 499-534.

[24] Zhao D and Reyhanoglu M, Feedback control of transient growth in a non-normal thermoacoustic system. Journal of Sound and Vibration (2014), 333, 3639-3656.

[25] Rubio-Hervas J, Zhao D and Reyhanoglu M, Nonlinear feedback control of thermoacoustic oscillations in a Rijke tube. Proceedings of IEEE International Symposium on Industrial Electronics (2014), 173–177.

[26] Rubio-Hervas J, Zhao D and Reyhanoglu M, Nonlinear feedback control of self-sustained thermoacoustic oscillations. Aerospace Science and Technology (2015), 41, 209-215.

[27] Zhao D and Li JW, Feedback control of combustion instabilities using a Helmholtz resonator with an oscillating volume. Combustion Science and Technology (2012), 184(5), 694-716.

[28] Rubio-Hervas J, Zhao D and Reyhanoglu M, Observer-based control of Rijke-type combustion instability. AIP Conference Proceedings (2014), 1637(1), 899-906.